M&C 2017 - International Conference on Mathematics & Computational Methods Applied to Nuclear Science & Engineering, Jeju, Korea, April 16-20, 2017, on USB (2017)

Advanced Analysis of Subcritical Neutron Noise Experiments

Erez Gilad*, Chen Dubi†, Benoit Geslot‡, Patrick Blaise‡

*The Unit of Nuclear Engineering, Ben-Gurion University of the Negev, Beer-Sheva 84105, Israel
†Department of Physics, Nuclear Research Center NEGEV (NRCN), Beer-Sheva 84190, Israel
‡DEN/CAD/DER/SPEx/LPE, CEA Cadarache, Saint-Paul-les-Durance 13108, France
gilade@bgu.ac.il

Abstract - *A novel method for direct and simultaneous estimation of the core kinetic parameters and its absolute reactivity is proposed. The method is based on the well known Feynman-Y method and is computationally intensive. The method does not rely on any pre-calculated or pre-measured physical quantity of the core, rather requires only the detector readings from an in-pile noise measurement and a set of delayed neutron group yields and the associated decay constants. The method is implemented and used for the analysis of subcritical configurations of the MAESTRO core in the MINERVE zero power reactor in order to measure its integral kinetic parameters,i.e., effective delayed neutron fraction β_{eff} and the prompt neutron generation time Λ, in addition to the absolute reactivity ρ. Uncertainty analysis shows that the associated uncertainties are reasonably small. Additionally, Feynman-Y curves are calculated for small time gates (down to 10^{-5} s), revealing an asymptotic approach to negative values. This is used to extract the detectors' dead time assuming that detector count losses due to dead time are the main contribution for this phenomenon. Finally, a new random sampling technique is proposed for obtaining Feynman-Y curve. The random sampling method has the advantages of producing less fluctuating curves and eliminating temporal correlations between successive time gates. Its major disadvantage is its dependence on CPU intense computations. Nonetheless, this method is implemented and compared to standard successive sampling technique.*

I. INTRODUCTION

A set of neutron noise measurements have been performed at the MINERVE zero power reactor at Cadarache research center in France [1] during September 2014. This experimental campaign was conducted in the framework of a tri-partite collaboration between CEA, PSI and SCK-CEN [2, 3]. These measurements were simultaneously and independently processed and analyzed in the framework of a collaboration between CEA, Ben-Gurion University of the Negev, and the Israeli Atomic Energy Commission. The main purpose of the campaign was to obtain the core kinetic parameters using various existing and novel noise techniques and compare it with recent measurements [4]. The last time a similar campaign was performed in MINERVE was in 1975 and the core configuration was different [5]. This campaign is a continuation of a previous campaign that aimed at determining the delayed neutron fraction β_{eff} in the MINERVE reactor using in-pile oscillations technique [6].

The MINERVE reactor is a pool-type (~120 m^3) reactor operating at a maximum power of 100 W with a corresponding thermal flux of 10^9 n/cm^2·s [1]. The core is composed of a driver zone, which includes 40 standard highly enriched MTR-type metallic uranium alloy plate assemblies surrounded by a graphite reflector. An experimental cavity, in which various UO_2 or MOX cladded fuel pins can be loaded in different lattices, reproducing various neutron spectra [1, 7], is located in the center of the driver zone. An oscillator piston, capable of moving periodically and vertically between two positions located inside and outside of the core is located inside the experimental zone. A general view of the MINERVE reactor is shown in Fig. 1, together with schematic drawings of the reactor geometrical configuration and the MAESTRO core configuration [8].

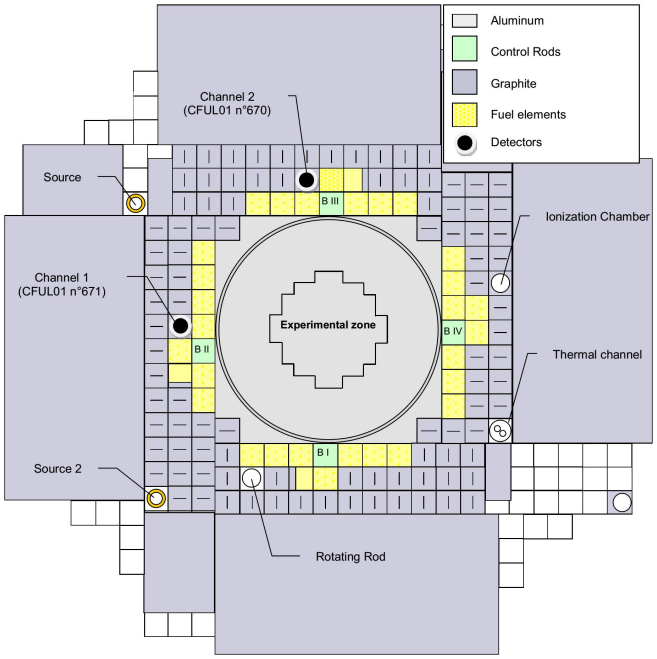

Figure 1. Experimental layout of the MINERVE during the noise measurements campaign in Sep. 2014.

During the measurement campaign, neutron noise experiments were conducted in two different subcritical states marked as "Acq16" and "Acq19". The different criticality states were obtained by inserting one of the four control rods

into the core. The reactor configuration was that of the MAESTRO program [8], representing a PWR spectrum in the central experimental cavity (see Fig. 1). Two large fission chambers with approximately 1g of ^{235}U have been installed next to the driver zone (denoted n°670 and n°671 in Fig. 1). In order to minimize flux disturbances in the detectors during measurement, reactor criticality was controlled by control rod B1, which is far from the two detectors. These subcritical measurements have been conducted at zero power with count rate around 4×10^4 cps. Both measurements lasted 5500 seconds and with core negative reactivity of 230 and 117 pcm, respectively, measured by pre-calibrated rod-drop experiment. The experimental configuration of the two subcritical measurements is summarized in Table I.

Table I. Pile noise measurements during the Sep. 2014 experimental campaign that are analyzed.

Data set	Acq16	Acq19
Control rod height [mm]	B1@399	B1@449
Core power [W]	0	0
Duration [s]	5500	5500
Integral fission rate F [s^{-1}]	4.28×10^9	8.43×10^9
Reactivity [pcm]	-230	-117

In this paper, a novel method is presented, which enables the *direct* and *simulaneous* estimation of three of the reactor core's integral parameters, e.g., the effective delayed neutron fraction β_{eff} the prompt neutron generation time Λ, and the core absolute reactivity ρ. The method is based on the well known Feynman-Y method [9, 10] and was previously applied to two parameters, β_{eff} and ρ [4].

Various new sampling techniques are proposed, studied, and implemented to obtain the variance-to-mean ratio curves, e.g., successive and random sampling of the detector's readings. The obtained curves are then fitted using a multi-mode delayed reactivity model, accounting for 1 prompt + 6 delayed neutron groups. Furthermore, analysis of the acquisition system dead time is pursued by studying the discrepancies between the Feynman-Y curves and the analytic models for small time gates, i.e., $T \lesssim 10^{-3}$ seconds.

Finally, the effect of the different sampling methods of the detectors' signal is studied. It is shown that random sampling methods, which eliminate the temporal correlations between adjacent time gates (is exist), produce slightly different results compared to the commonly and widely used successive sampling technique. Different random sampling techniques are proposed, implemented, and analyzed.

II. THE FEYNMAN-Y METHOD

Each point on the Feynman-Y curve is obtained in the following manner. Each measurement of a total duration $\tilde{T}$ is divided into N_T segments (or time gates) of duration T (where $N_T = \tilde{T}/T$). Define a series of random variables $\{X_T(n)\}_{n=1}^{N_T}$, where $X_T(n)$ is the number of neutron detections in the n^{th} segment. The expectation value $E(X_T)$ and the variance $Var(X_T)$ are evaluated, where the Feynman-Y function (the variance to mean ratio) is defined by:

$$Y(T) = \frac{Var(X_T)}{E(X_T)} - 1 \ . \tag{1}$$

Once the Feynman-Y curve is obtained, the data is fitted on an analytic expression, from which the reactivity, the delayed neutron fraction or the neutron generation time can be estimated. Two analytic models for the Feynman-Y are usually used: with and without an explicit reference to the delayed neutrons. To simplify notations, the model neglecting the effect of the delayed neutrons is refererred to as the Prompt Reactivity Analysis (PRA), and the model incorporating the delayed neutrons is referred to as the Delayed Reactivity Analysis (DRA) [4].

1. Prompt Reactivity Analysis (PRA)

The most basic fit model [9], the PRA model, is given by:

$$Y(T) = Y_\infty \times \left(1 - \frac{1 - e^{-\alpha_p T}}{\alpha_p T}\right) \ , \tag{2}$$

where $\alpha_p \equiv \frac{\beta_{\text{eff}} - \rho_p}{\Lambda}$, ρ_p is the prompt reactivity, β_{eff} is the delayed neutron fraction and Λ is the prompt neutron generation time. Eq. (2) is the single energy point-wise prompt neutrons model [11] and it is only applicable for $T < 0.1$ s.

2. Delayed Reactivity Analysis (DRA)

A generalization of Equation (2) to a 1-prompt and 6-delayed neutron groups [12, 13] can be written in the following form:

$$Y(T) = C \times \sum_j^7 \frac{2A_j}{\alpha_j} H_0(\alpha_j)\left(1 - \frac{1 - e^{-\alpha_j T}}{\alpha_j T}\right) \ , \tag{3}$$

where the coefficients A_j are determined by the transfer function

$$H_0(\omega) = \frac{1 - i\omega\left(\sum_{k=1}^6 \frac{\beta_k}{\lambda_k + i\omega}\right)}{i\omega\left(\Lambda + \sum_{k=1}^6 \frac{\beta_k}{\lambda_k + i\omega}\right) - \rho} = \sum_{j=1}^7 \frac{A_j}{i\omega + \alpha_j} \tag{4}$$

and the coefficients α_j are the roots of the Inhour equation

$$-\alpha_j\left(\Lambda + \sum_{k=1}^6 \frac{\beta_k}{\lambda_k - \alpha_j}\right) - \rho = 0 \ . \tag{5}$$

Notice that although Eq. (4) has a large number of parameters, the fit is done using two parameters, i.e. ρ and C. Moreover, once the roots of the Inhour equations are found, the residua A_j are given explicitly by

$$A_j = \frac{1 - \left(\sum_{k=1}^6 \frac{\alpha_j \beta_k}{\lambda_k + \alpha_j}\right)}{\Lambda + \sum_{k=1}^6 \frac{\lambda_k \beta_k}{(\lambda_k - \alpha_j)^2}} \ . \tag{6}$$

In the DRA model the procedure is a bit more complicated since the dependence of $Y(T)$ on ρ is implicit (via Eqs. 4–6).

By denoting $\beta_{\text{eff}} = \sum_{j=1}^{6} \beta_j$ and $\varepsilon_j = \beta_j/\beta_{\text{eff}}$, Eq. (4) may be rewritten in the following form

$$H_0(\omega) = \frac{1 - i\omega\beta_{\text{eff}} \left(\sum_{k=1}^{6} \frac{\varepsilon_k}{\lambda_k + i\omega} \right)}{i\omega \left(\Lambda + \beta_{\text{eff}} \sum_{k=1}^{6} \frac{\varepsilon_k}{\lambda_k + i\omega} \right) - \rho} \ , \tag{7}$$

and the Inhour equation (Eq. 5) as

$$-\alpha_j \left(\Lambda + \beta_{\text{eff}} \sum_{k=1}^{6} \frac{\varepsilon_k}{\lambda_k - \alpha_j} \right) - \rho = 0 \ . \tag{8}$$

Thus, assuming that ε_j are known (e.g., [14]), it is possible to link between the kinetic parameters and the reactivity using curve fitting.

Note that for both models, one usually assumes knowledge of two of the three parameters ρ, β_{eff}, and Λ, in order to estimate the third parameter. This can be done either by calculation or by experimental measurement, leaving the third parameter as a degree of freedom to be evaluated using the Feynman-Y curve fitting.

III. RESULTS AND ANALYSIS

1. Direct Estimation of Integral Parameters

Usually, in order to calculate some integral kinetic parameter of the core, the other parameters, including the core reactivity, are assumed to be known (e.g., previously measured or calculated). For example, in order to evaluate β_{eff}, the core reactivity ρ and the prompt neutron lifetime Λ need to be known. Gilad et al. [4] showed that it is possible to simultaneously evaluate both ρ and β_{eff}, assuming a global minimum exists over the two-dimensional parameter space for the error in the multidimensional fits. The obtained curves using this method exhibit better agreement with the observed results with respect to the curves obtained using the pre-calculated reactivity, as shown in Fig. 2.

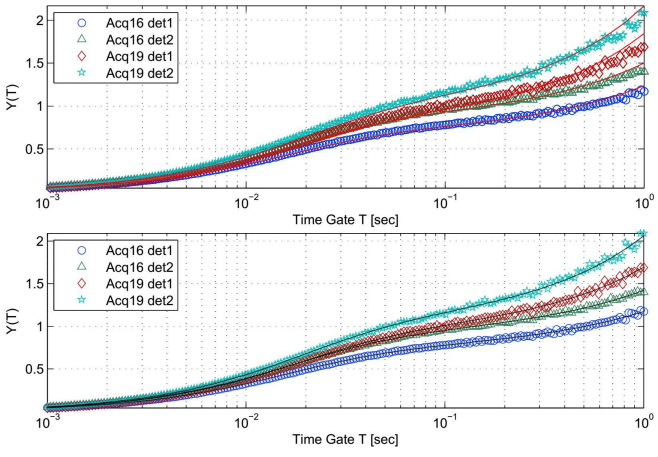

Figure 2. The Feynman-Y curves for both detectors in both subcritical experiments and the corresponding best fitted curves obtained by using the given ρ (solid red lines) and the global minimum in the (ρ,β_{eff}) parameter space [4].

In this paper, all three parameters, i.e., ρ, β_{eff}, and Λ are simultaneously fitted and the best fit over the $(\rho, \beta_{\text{eff}}, \Lambda)$ parameter space is obtained, assuming global minimum exists for the fit error. The error in the fit is evaluated for each point in the $(\rho, \beta_{\text{eff}}, \Lambda)$ parameter space by the sum of the squares of the differences between the measured data and the fitted Feynman-Y curve. The error is calculated according to the following formula

$$e^2(\rho, \beta_{\text{eff}}, \Lambda) = \sum_{l=1}^{N} \left[FY_l - Y\left(T_l | \rho, \beta_{\text{eff}}, \Lambda\right) \right]^2 \ , \tag{9}$$

where FY_l is a measured data point l and $Y\left(T_l | \rho, \beta_{\text{eff}}, \Lambda\right)$ is the fitted curve for given (ρ,β_{eff},Λ) set of values, evaluated at point T_l.

It was already shown [4] that this error's behavior over the $(\rho, \beta_{\text{eff}})$ parameter space exhibits a global minimum, which enables the simultaneous estimation of both ρ and β_{eff}. It is shown that the error defined in Eq. (9) exhibits a global minimum also in the three-dimensional space (ρ,β_{eff},Λ), enabling the *direct* and *simultaneous* estimation of ρ, β_{eff}, and Λ without the need for preliminary measurements. The error behavior over the three-dimensional parameter space (ρ,β_{eff},Λ) is shown in Figs. 3, 4, and 5.

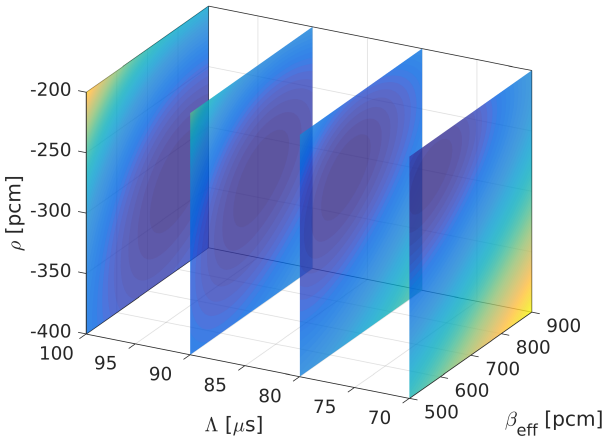

Figure 3. The error in the multidimensional fit, as defined in Eq. (9), over the three-dimensional parameter space (ρ,β_{eff},Λ), shown at constant Λ cross sections. The error values range between 0.008 (dark blue) and 0.7 (yellow).

The best fitted curves obtained using this method are shown in Fig. 6. The obtained curves show good agreement with the measured data with no significant biasing in the normalized residuals. It should be noted that non of the parameters were calculated or measured prior to the analysis. Rather, they are evaluated simultaneously and directly from the detector's readings, which is the only measured input for this method. It should be noted that spatial higher mode components of Y values were not corrected [15].

This method provides not only the best estimate for ρ, β_{eff}, and Λ, but also a measure for the uncertainties associated with the values of these parameters, originating from

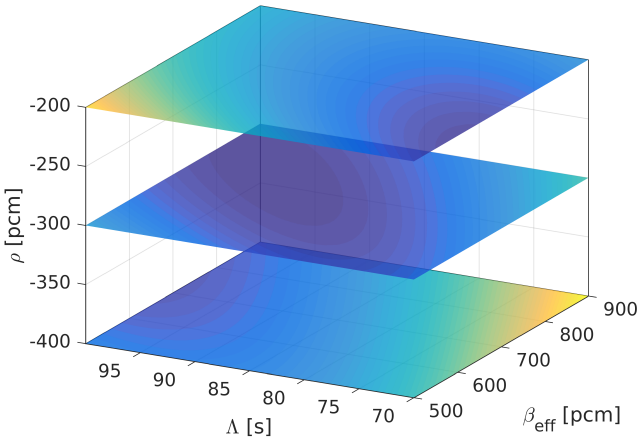

Figure 4. The error in the multidimensional fit, as defined in Eq. (9), over the three-dimensional parameter space (ρ,β_{eff},Λ), shown at constant reactivity ρ cross sections. The error values range between 0.008 (dark blue) and 0.7 (yellow).

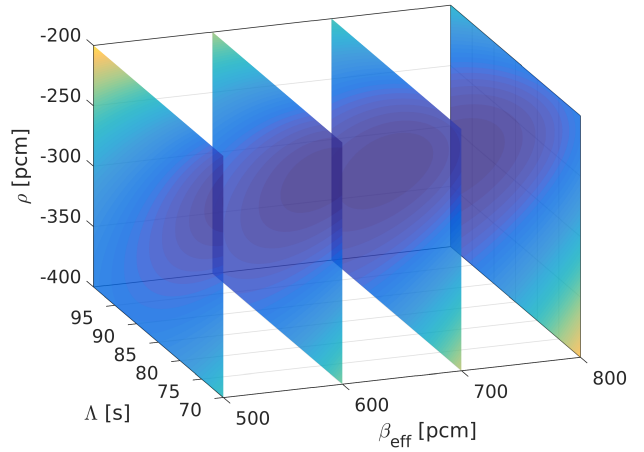

Figure 5. The error in the multidimensional fit, as defined in Eq. (9), over the three-dimensional parameter space (ρ,β_{eff},Λ), shown at constant β_{eff} cross sections. The error values range between 0.008 (dark blue) and 0.7 (yellow).

the correlations between the core reactivity and the kinetic parameters. Just as the values of these parameters are obtained from the location of the global minimum of the error in the three-dimensional parameter space (ρ,β_{eff},Λ), the associated uncertainties can be evaluated by examining its near surroundings.

Let us mark the point of global minimum of the fit error e^2 (Eq. 9) in the parameter space (ρ,β_{eff},Λ) by $\boldsymbol{r_0}$. Any deviation from the global minimum, in any direction, i.e., $\boldsymbol{r_0} + d\boldsymbol{r}$, is bound to increase the error in the fit. Hence, for any small number ϵ, there exist a connected closed surface in the parameter space which encloses a volume in which the error in the fit is bounded by ϵ, i.e., $e^2(\boldsymbol{r_0} + d\boldsymbol{r}) \leqslant e^2(\boldsymbol{r_0}) + \epsilon$. Two dimensional cross sections of this volume for different values

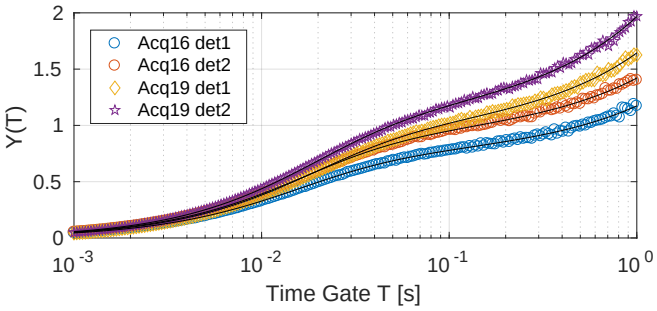

Figure 6. Feynman-Y curves for both detectors in both subcritical experiments and the corresponding best fitted curves obtained by using multidimensional fit (solid black lines) and the global minimum in the (ρ,β_{eff},Λ) parameter space.

of ϵ are shown in Fig. 7. The values of ϵ in these figures are set such that they bound volumes of 1–5% increase in the minimal fit error $e^2(\boldsymbol{r_0})$.

This procedure for estimating the associated uncertainties in the core reactivity and the kinetic parameters has the advantage of accounting for the complex correlations between these physical quantities. Examination of Fig. 7 reveals that β_{eff} is the most sensitive parameter with respect to the fit error (in terms of absolute sensitivity). An increase of 1% in the fit error can change β_{eff} by 10–15 pcm, whereas Λ is changed by 1 μs and ρ by 3–6 pcm.

The kinetic parameters and the core reactivity along with their associated uncertainties (taken at 1%) are summarized in Table II.

Data set	ρ [pcm]	β_{eff} [pcm]	Λ [μs]
Acq16 det1	-301±6 (±2.0%)	750±15 (±2.0%)	92.5±1 (±1.0%)
Acq16 det2	-312±6 (±1.9%)	726±15 (±2.0%)	95.5±1 (±1.0%)
Acq19 det1	-222±6 (±2.7%)	703±15 (±2.1%)	98.0±1 (±1%)
Acq19 det2	-199±6 (±3.0%)	742±15 (±2.0%)	100.0±1 (±1%)

Table II. The kinetic parameters and the core reactivity, obtained using the global minimum method described above, along with their absolute and relative (in parentheses) associated uncertainties (taken at 1% change in the fit error e^2).

2. Dead Time Effect

Usually, the minimal time gate width considered for prompt and delayed models is ~10^{-3} s. However, when examining the behavior of the measured Feynman-Y curves and comparing them to the analytic models for small time gates, i.e., in the interval [10^{-5},10^{-3}] seconds, discrepancies emerge [16–18], as shown in Fig. 8. While the models asymptotically approach zero, the measured Feynman-Y curves does not. This behavior is observed in all our subcritical measure-

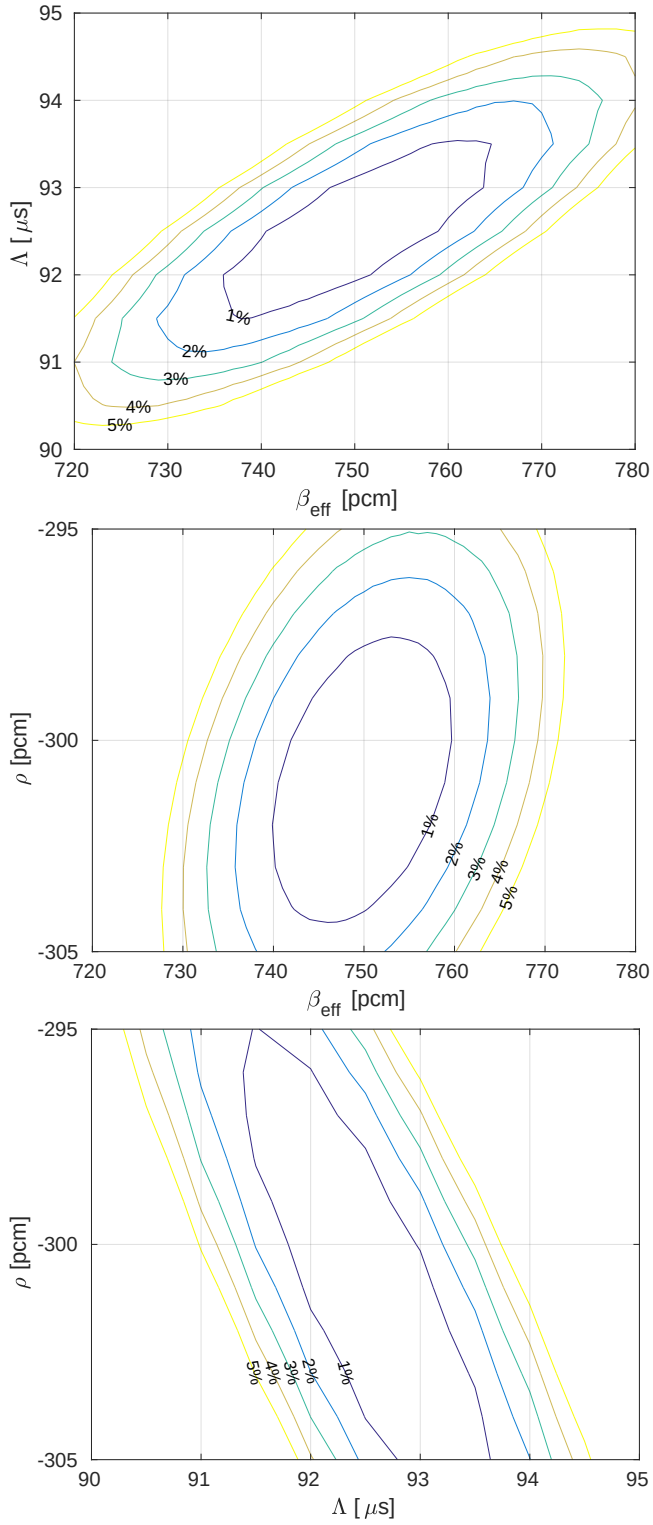

Figure 7. Two dimensional cross section of the volumes in the parameter space for which the fit error e^2 is increased by 1–5%. The cross sections are taken through the global minimum $\boldsymbol{r_0}$.

ments.

The fact that the measured Feynman-Y curves asymptotically approach negative values for small time gates is indicative of the count losses due to detector dead time [11, 16, 17, 19–21]. According to these references, the non-correlated part of the variance-to-mean ratio depends linearly on the dead time according to

$$Y_\tau(T) = Y(T) - 2R\tau \ , \tag{10}$$

where $Y(T)$ is either the prompt or delayed variance-to-mean formula given in Eqs. (2) and (3), R is the mean count rate, and τ is the dead time of the acquisition system. Hence, as T, decreases, $Y(T) \to 0$ and the expression for τ approaches $\tau = Y_\tau(T)/2R$. The evaluated effective dead times for the different measurements and the different detectors are summarized in Table III.

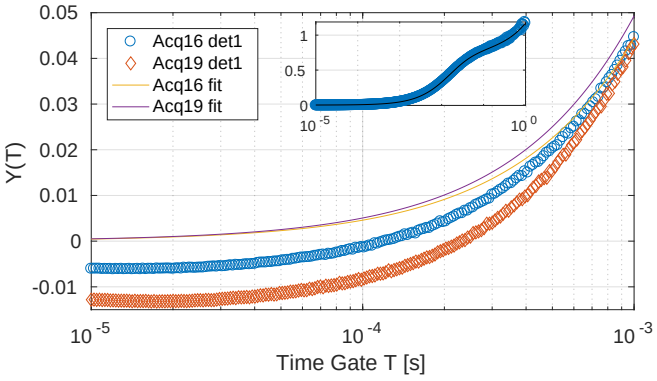

Figure 8. The discrepancies between the asymptotic behavior of the analytic models and the measured Feynman-Y curves as the time gates decrease. The inset shows the full range of the Feynman-Y curves.

Dead time [ns]	det1	det2
Acq16	78	77
Acq19	87	88

Table III. Estimated values for the detectors' dead time using the Feynman-Y curves for small time gates (see Fig. 8).

It should be noted that for such small time gates, i.e., less than 100 μs, the fact that the Feynman-Y curves assume negative values can also be indicative of other effects in addition to count losses due to dead time, e.g., temporal correlations between adjacent time gates.

3. Random vs. Successive Sampling Techniques

The conventional sampling technique for Feynman-Y curves calculations is successive sampling of the detector signal [22, 23]. For each time gate T, the signal is divided into successive (non-overlapping) segments of data, as illustrated in Fig. 9. The variance and mean values of the detector counts for each time gate T are calculate for each segment.

The successive sampling technique has the clear advantages of simple implementation and fast execution, but is obviously biased due to temporal correlations between successive segments. However, the effect of this bias on the Feynman-Y method is rather unclear. In short, opinions on this issue range

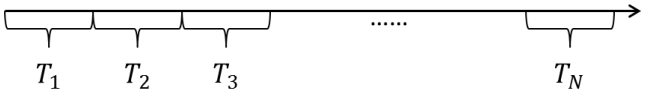

Figure 9. Illustration of a conventional successive sampling.

between the need to change the basic classic equation (Eq. 2) so it accounts for these correlations, through the proposition to insert waiting times between successive time gates to reduce the correlations' effect, and the statement that there are no experimental evidence for the existence of these correlations (see discussion in ref. [11] page 62).

In order to study this effect (and out of pure curiosity), a random sampling technique is applied to the signal. A single detection time is chosen uniformly at random and a time gate T is opened from that point. This process is repeated a variable number of times, depending on the time gate T and on the requirement that on average most detections are sampled. This sampling method has an obvious bias, since each time gate starts with a detection. Moreover, overlapping is allowed, as illustrated in Fig. 10. If temporal correlations exist between successive time gates and affect the Feynman-Y analysis, than this type of sampling should eliminate this effect.

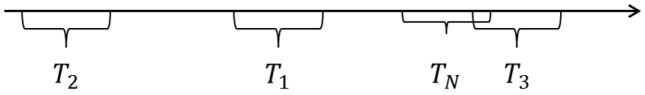

Figure 10. Illustration of a random sampling.

A comparison of Feynman-Y curves obtained (from the same data) by using conventional successive sampling and by using different random sampling techniques is shown in Fig. 11. Overall, the different Feynman-Y curves seem to overlap for most time gates. The middle panel shows that random sampled curves with large number of samples per time gate (rand1, rand2, rand3) exhibit less fluctuating behavior with respect to other curves. The bottom panel shows that the random sampling curves deviate from the successive sampling one for small time gates, starting from $T \lesssim 10^{-2}$ s. This behavior is exhibited in all our subcritical measurements for all detectors.

The different random sampling curves differ only in the number of segments chosen randomly for each T, i.e., the rand0 curve is calculated using the same number of successive segments per T, the rand1 curve is calculated using 10^5 segments per T, the rand2 curve is calculated using 10 times the number of successive segments per T, and the rand3 curve is calculated using the larger number of segment between rand1 and rand2 per T.

Preliminary analysis suggest that the sampling technique has a notable effect on the fit results of the Feynman-Y method. However, the deviation of the random sampled curves from the successive sampled one for small time gates may indicate an insufficient number of samples used. If that is the case, variance-to-mean values are obtained using only part of the available data and may be prone to errors. The results are summarized in Table IV.

The analysis was performed using the global minimum method described above. Comparison of the results to those

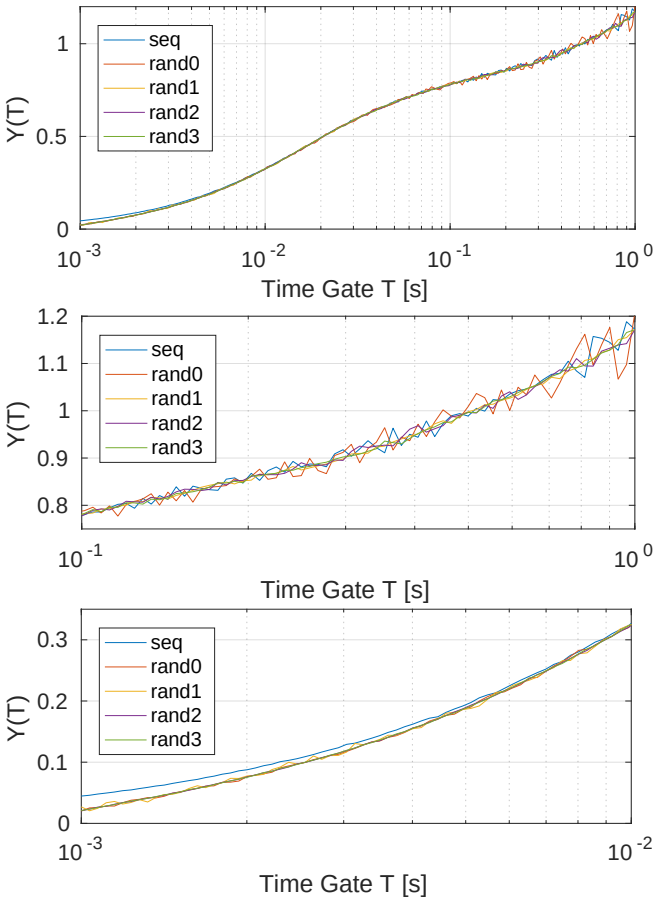

Figure 11. Feynman-Y curves obtained using successive and random sampling (Acq16, det1). The top panel illustrates the range $[10^{-3},10^{0}]$ s, whereas the middle and bottom panels zoom-in on the range $[10^{-1},10^{0}]$ and $[10^{-3},10^{-2}]$ s, respectively.

given in Table II shows that both rand1 and rand3 seems reliable, whereas rand0 and rand2 tend to deviate from the values obtained by successive sampling, especially underestimating β_{eff}.

IV. CONCLUSIONS

A novel method for *direct* and *simultaneous* estimation of the core kinetic parameters and its absolute reactivity is presented. The method is based on the well known Feynman-Y method and is computationally intensive. The method does not rely on any pre-calculated or pre-measured physical quantity of the core, rather requires only the detector readings from an in-pile noise measurement and a set of delayed neutron group yields and the associated decay constants. Thus, this novel approach eliminates the need for *prior* reactivity calibrations, e.g., rod-drop or stable period analysis.

The method is implemented and used for the analysis of subcritical configurations of the MAESTRO core in the MINERVE zero power reactor in order to measure its integral kinetic parameters,i.e., effective delayed neutron fraction β_{eff} and the prompt neutron generation time Λ, in addition to the absolute reactivity ρ. It is found that the results obtained

		ρ [pcm]	β_{eff} [pcm]	Λ [μs]
Acq16 det1	rand0	-297	698	91.0
	rand1	-307	720	93.5
	rand2	-293	680	89.0
	rand3	-308	725	94.0
Acq16 det2	rand0	-287	722	94.5
	rand1	-310	712	96.5
	rand2	-289	682	91.5
	rand3	-314	726	98.0
Acq19 det1	rand0	-212	680	95.5
	rand1	-225	710	100.0
	rand2	-220	694	97.5
	rand3	-225	710	100.0
Acq19 det2	rand0	-202	724	100.0
	rand1	-200	721	98.4
	rand2	-200	728	99.5
	rand3	-203	730	100.1

Table IV. The kinetic parameters and the core reactivity, obtained using the global minimum method described above, using different random sampling techniques of the detector signal.

using this method closely resemble results that were obtained using a one-d and two-imensional fits on the β_{eff} parameter where both ρ and Λ were calculated and measured prior to the analysis [2, 3]. This method is a generalization of the method proposed by [4] in which only Λ was calculated prior to the analysis and both β_{eff} and ρ were simultaneously fitted.

This method provides not only the best estimate for ρ, β_{eff}, and Λ, but also a measure for the uncertainties associated with the values of these parameters, originating from the correlations between the core reactivity and the kinetic parameters. The procedure for estimating the associated uncertainties in the core reactivity and the kinetic parameters has the advantage of accounting for the complex correlations between these physical quantities. The Uncertainty analysis shows that the associated uncertainties are reasonably small (1–3% for all parameters), and that β_{eff} is the most sensitive parameter with respect to the fit error (in terms of absolute sensitivity).

The effect of count losses due to detector's dead time was examined by calculating the Feynman-Y curves for small time gates (down to 10^{-5} s), revealing an asymptotic approach to negative values. This is used to obtain the detectors' dead time assuming that detector count losses due to dead time are the main contribution for this phenomenon. The experimental measurements were performed in zero power and relatively low count rates, but the effect of the dead time, although small, is still detectable,

Finally, a new random sampling technique is proposed, in various configurations, for obtaining Feynman-Y curve. The random sampling method has the advantages of producing less fluctuating curves and eliminating temporal correlations between successive time gates. Its major disadvantage is its dependence on CPU intense computations. Nonetheless, this method is implemented and compared to standard successive sampling technique. It is shown that Feynman-Y curves obtained by random sampling techniques deviate from the ones obtained by conventional successive sampling for small time gates, which might result from the fact that random sampling eliminate temporal correlation between successive data segments. However, it may also indicate an insufficient number of samples used. If that is the case, variance-to-mean values are obtained using only part of the available data and may be prone to errors.

REFERENCES

1. G. BIGNAN, P. FOUGERAS, P. BLAISE, J.-P. HUDELOT, and F. MELLIER, "Reactor Physics Experiments on Zero Power Reactors," in D. G. CACUCI, editor, "Handbook of Nuclear Engineering," Springer, vol. III, chap. 18, pp. 2084–2109 (2010).

2. B. GESLOT, A. GRUEL, A. PEPINO, J. D. SALVO, G. DE IZARRA, C. JAMMES, C. DESTOUCHES, and P. BLAISE, "Pile noise experiment in MINERVE reactor to estimate kinetic parameters using various data processing methods," in "4th ANIMMA, 20-24 April 2015, Lisbon," (2015).

3. G. PERRET, "Delayed neutron fraction and prompt decay constant measurement in the MINERVE reactor using the PSI instrumentation," in "4th ANIMMA, 20-24 April 2015, Lisbon," (2015).

4. E. GILAD, A. KOLIN, O. RIVIN, C. DUBI, B. GESLOT, and P. BLAISE, "Analysis of critical and subcritical neutron noise experiments in MINERVE using advanced noise techniques," in "PHYSOR 2016, Sun Valley, Idaho, May 1-5," (2016).

5. J. CARRE and J. D. C. OLIVEIRA, "Measurements of kinetic parameters by noise techniques on the MINERVE reactor," *Annals of Nuclear Energy*, **2**, *2*, 197– 206 (1975).

6. E. GILAD, O. RIVIN, H. ETTEDGUI, I. YAAR, B. GESLOT, A. PEPINO, J. D. SALVO, A. GRUEL, and P. BLAISE, "Experimental estimation of the delayed neutron fraction of the MAESTRO core in the MINERVE zero power reactor," *Journal of Nuclear Science and Technology*, **52**, *7-8*, 1026–1033 (2015).

7. J. PASCAL HUDELOT, R. KLANN, P. FOUGERAS, F. JORION, N. DRIN, and L. DONNET, "OSMOSE: An Experimental Program for the Qualification of Integral Cross Sections of Actinides," in "PHYSOR 2004, Chicago, Illinois, April 25-29," (2004).

8. P. LECONTE, B. GESLOT, A. GRUEL, A. PEPINO, M. DERRIENNIC, J. DI-SALVO, M. ANTONY, R. ESCHBACH, and S. CATHALAU, "MAESTRO: An ambitious experimental programme for the improvement of nuclear data of structural, detection, moderating and absorbing materials - First results for nat V, ^{55}Mn, ^{59}Co and ^{103}Rh," in "3rd ANIMMA, 23-27 June 2013, Marseille, France," (2013).

9. R. P. FEYNMAN, "Statistical behavior of neutron chains," Tech. rep., Los Alamos (1946).

10. R. FEYNMAN, F. D. HOFFMANN, and R. SERBER, "Dispersion of the neutron emission in U-235 fission," *Journal of Nuclear Energy*, **3**, *1*, 64–69 (1956).

11. R. E. UHRIG, *Random noise techniques in nuclear reactor systems*, Ronald Press Company (1970).

12. E. F. BENNETT, "The rice formulation of pile noise," *Nuclear Science and Engineering*, **8**, *1*, 53–61 (1960).

13. J. THIE, *Reactor Noise*, ANS and U.S. AEC Monograph Series on nuclear science and technology, Rowman and Littlefield (1963).

14. G. R. KEEPIN, *Physics of Nuclear Kinetics*, Addison-Wesley (1965).

15. T. YAMAMOTO, "Higher order mode analyses in Feynman-α method," *Annals of Nuclear Energy*, **38**, *6*, 1231–1237 (2011).

16. K. HASHIMOTO, K. OHYA, and Y. YAMANE, "Experimental investigations of dead-time effect on Feynman-α method," *Annals of Nuclear Energy*, **23**, *14*, 1099–1104 (1996).

17. J. KLOOSTERMAN and Y. RUGAMA, "Feynman-α measurements on the fast critical zero-power reactor masurca," *Progress in Nuclear Energy*, **46**, *2*, 111–125 (2005).

18. C. BERGLÖF, M. FERNÁNDEZ-ORDÓÑEZ, D. VILLAMARÍN, V. BÉCARES, E. M. GONZÁLEZ-ROMERO, V. BOURNOS, and J.-L. MUÑOZ-COBO, "Auto-correlation and variance-to-mean measurements in a subcritical core obeying multiple alpha-modes," *Annals of Nuclear Energy*, **38**, *2–3*, 194–202 (2011).

19. Y. YAMANE and D.-I. ITO, "Feynman-α formula with dead time effect for a symmetric coupled-core system," *Annals of Nuclear Energy*, **23**, *12*, 981–987 (1996).

20. Y. YAMANE, T. MISAWA, S. SHIROYA, and H. UNESAKI, "Formulation of data synthesis technique for Feynman-α method," *Annals of Nuclear Energy*, **25**, *1*, 141–148 (1998).

21. E. WALLERBOS and J. HOOGENBOOM, "The forgotten effect of the finite measurement time on various noise analysis techniques," *Annals of Nuclear Energy*, **25**, *10*, 733–746 (1998).

22. Y. KITAMURA, M. MATOBA, T. MISAWA, H. UNESAKI, and S. SHIROYA, "Reactor noise experiments by using acquisition system for time series data of pulse train," *Journal of Nuclear Science and Technology*, **36**, *8*, 653–660 (1999).

23. R. OKUDA, A. SAKON, S. YA HOHARA, W. SUGIYAMA, HIROSHI, TANINAKA, and K. HASHIMOTO, "An improved Feynman-α analysis with a moving-bunching technique," *Journal of Nuclear Science and Technology*, **53**, *10*, 1647–1652 (2016).